Cross-Beam Energy Transfer in Polar-Drive Implosions on OMEGA

In the direct-drive approach to inertial confinement fusion, laser beams directly illuminate a spherical target, depositing their energy in the coronal plasma. This energy is transported to higher densities where ablation occurs and material rapidly expands, driving the nuclear fuel toward the center of the capsule. Symmetric illumination is required to produce a spherically symmetric drive. Ideally, the target is illuminated by a sufficient number of beams, distributed symmetrically around the target, to provide an adequately uniform drive with sufficient pressure to achieve ignition.[1]

In the current x-ray drive configuration of the National Ignition Facility (NIF),[2] there are no laser beams near the equator of the target chamber and direct-drive experiments are performed in the polar-drive (PD) geometry.[3] PD creates a uniform implosion by combining and repointing the NIF beams toward the target equator, employing phase plates designed to create specific on-target spot sizes, pulse shaping, and shimming of the target layers.[4] The coupling of laser energy into the target can be decreased by cross-beam energy transfer (CBET)[5–7] between the lasers.

CBET occurs when laser light seeds stimulated Brillouin scattering (SBS) in a plasma by crossing two or more laser beams. This low-gain SBS can drive ion-acoustic waves and transfer a significant amount of energy from one of the crossing beams to the other. Hydrodynamic one-dimensional (1-D) modeling of symmetric 60-beam direct-drive implosions on OMEGA that do not include CBET physics overpredict the laser drive by 10% to 20% as indicated by discrepancies with the observed bang times and time-dependent scattered-light spectra.[8–10] Recently it was shown that decreasing the laser beams' radius with respect to the target radius reduces CBET and improves fusion yields.[11] The incorporation of CBET physics into the 1-D hydrodynamic modeling of symmetrically illuminated implosions produces good agreement with the observables, but the large scattering angles and three-dimensional (3-D) nature of the PD geometry has prevented previous CBET models from quantifying CBET in PD implosions.

CBET has been identified as a mechanism responsible for transferring significant amounts of energy between the NIF beams in indirect-drive hohlraum experiments.[6] Independently varying the wavelength of the NIF beams to control CBET is used to tune the implosion symmetry.[12] CBET in indirect-drive experiments occurs at relatively low densities and the angle between crossing beams is small, so the models that post-process the hydrodynamic simulations to calculate CBET can use a paraxial approximation.[6,7,13]

This article presents the first measurements of the effects of CBET in PD. The angular dependence of the unabsorbed light is measured to decrease from 1200 J/sr on the pole to 200 J/sr along the equator. These measurements and those of the unabsorbed light intensity and the spectra are reproduced by 3-D CBET modeling. These results indicate that CBET in PD reduces the absorbed energy by 10%. This reduction in absorption is consistent with the measurement of the bang time, which is ~180 ps later than predicted when CBET modeling is not included.[14] Calculations indicate that the drive symmetry is reduced by energy transferred from the center of beams pointed near the equator to the outer edge of the beams pointed near the pole. This drive symmetry can be recovered by shifting the relative wavelength of the beams in each cone but the overall reduction in absorption is not ameliorated. The model predicts that CBET can be mitigated by using smaller beam spots.

The CBET calculations in this polar-drive geometry were carried out by post-processing two-dimensional (2-D) hydrodynamic simulations using a 3-D CBET model. The time-varying coronal plasma parameters were calculated by the code *DRACO*,[15] where a Spitzer–Härm heat-transport model was used that limits the heat flow to a fraction ($f = 0.06$) of the free-streaming flux.[16] The PD beam profiles in the CBET model are treated as the sum of many beamlets where the path and Doppler-shifted wavelength of each beamlet through the corona are determined by 3-D ray tracing (Fig. 133.29). This is a major difference between modeling CBET for polar drive and previous work modeling indirect-drive CBET, where the

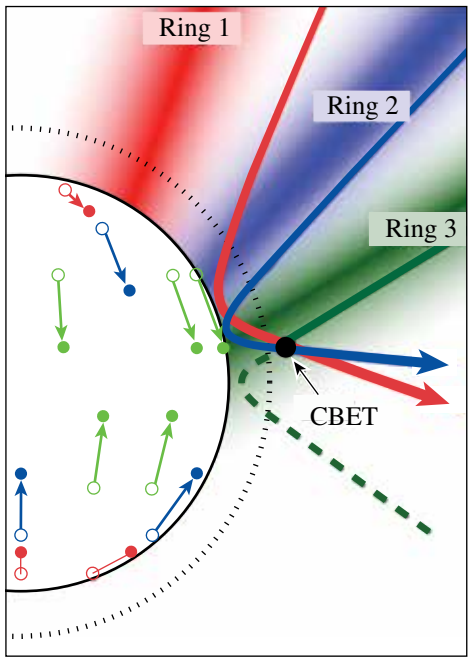

Figure 133.29
Pointing offsets for the beam rings for the polar-drive (PD) implosions on OMEGA used in this article: Ring 1 (red), Ring 2 (blue), and Ring 3 (green). Open circles show the pointing of each ring in symmetric drive (i.e., toward target chamber center); closed circles show the repointed PD geometry. The beamlets (rays) in the corona illustrate the effect of cross-beam energy transfer (CBET) on the laser illumination. The green Ring 3 beamlet directed toward the target equator is crossed by outgoing beamlets from Rings 1 and 2 before it reaches its nearest approach to the ablation surface, where it will be strongly absorbed. CBET scatters energy from this equatorial beamlet to the outgoing beamlets, reducing the energy deposition at the equator near the ablation surface.

refraction of the laser beams is ignored.[13] The CBET at crossings between beamlets for all PD beams is calculated from the SBS spatial gain length in the strong damping limit.[9,17]

The PD implosions used 40 ultraviolet (λ_0 = 351 nm) OMEGA laser beams.[18] In the PD geometry, the beams are grouped into three rings with offset pointing toward the target equator as shown in Fig. 133.29. The laser beams were smoothed by polarization smoothing,[18] distributed phase plates,[19] and smoothing by spectral dispersion.[20] All beams used the same pulse shape and distributed phase plates with circular super-Gaussian ($n = 4$) beam profiles, where 95% of the power is within a diameter of 865 μm. The beams were incident on spherical CH capsules with 27-μm-thick walls and a total diameter of 866 μm. The targets were filled with 11.4 atm of D_2.

The angular dependence of the unabsorbed light was measured using 12 calorimeters located around the target chamber [Fig. 133.30(a)]. Four of these locations couple the unabsorbed light to a 1.25-m spectrometer with a Rochester Optical Streak System via optical fibers. This system has a spectral resolution of 0.05 nm and a temporal resolution of 90 ps.

Figure 133.30(b) shows the time-integrated angular distribution of the light that is scattered (i.e., not absorbed) by the coronal plasma. A factor-of-6 more light is measured on the pole than the equator. This is in good agreement with calculations of the unabsorbed light when using the CBET model, and Fig. 133.30(b) shows that the unabsorbed light at all angles is significantly underestimated when the CBET model is not used.

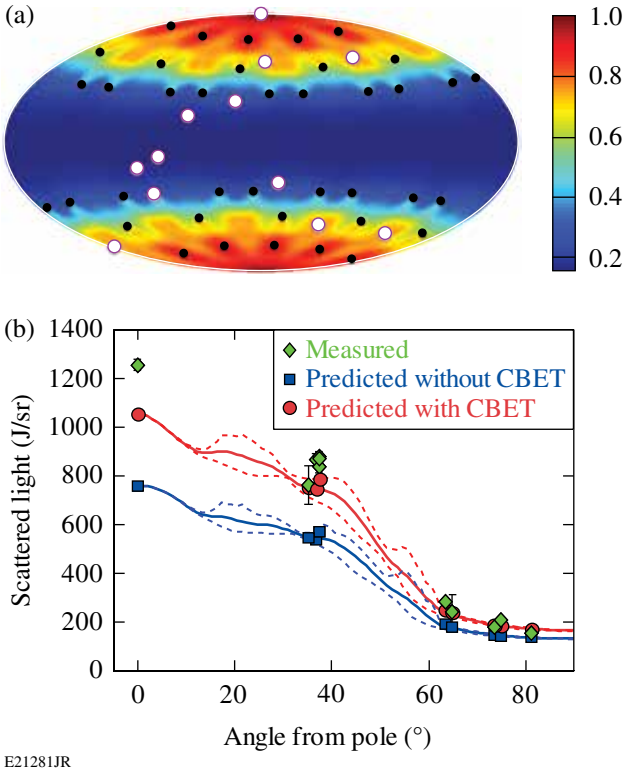

Figure 133.30
(a) Aitoff projection of the calculated distribution of the normalized time-integrated scattered light over the inner surface of the OMEGA target chamber. White circles show the locations of the scattered-light calorimeters in the OMEGA chamber. Black dots represent the beam ports. (b) Time-integrated, unabsorbed-light radiant intensity as a function of angle from the PD symmetry axis as predicted without CBET modeling (blue squares), predicted with CBET modeling (red circles), and measured (green diamonds). The error bars on the measurements are the standard deviation of multiple measurements from nominally identical PD implosions. The solid lines show the model calculations of the mean value of the radiant intensity, while the dashed lines show the calculated minimum/maximum range around the target azimuthally.

Figure 133.31 shows that, in addition to the total integrated scattered power, the CBET model accurately predicts the time-varying spectrally resolved details of unabsorbed light from the PD implosions. The measured spectra from two polar angles [Figs. 133.31(a) and 133.31(b)] show the variation in wavelength and power of the unabsorbed light. This variation is the result of the time-varying optical path length of the light traveling through the coronal plasma. The initial blue shift in the spectra occurs as the light propagates through a rapidly increasing electron density when the plasma is formed.[21] The blue shift results partially from the outward movement of the plasma's critical-density surface (a moving-mirror Doppler shift) and partially from the outward buildup of the coronal plasma that reduces the optical path length of the laser light because plasma has a smaller index of refraction than vacuum. As the plasma scale length reaches a steady state, the plasma's critical-density surface implodes, red shifting the unabsorbed light.

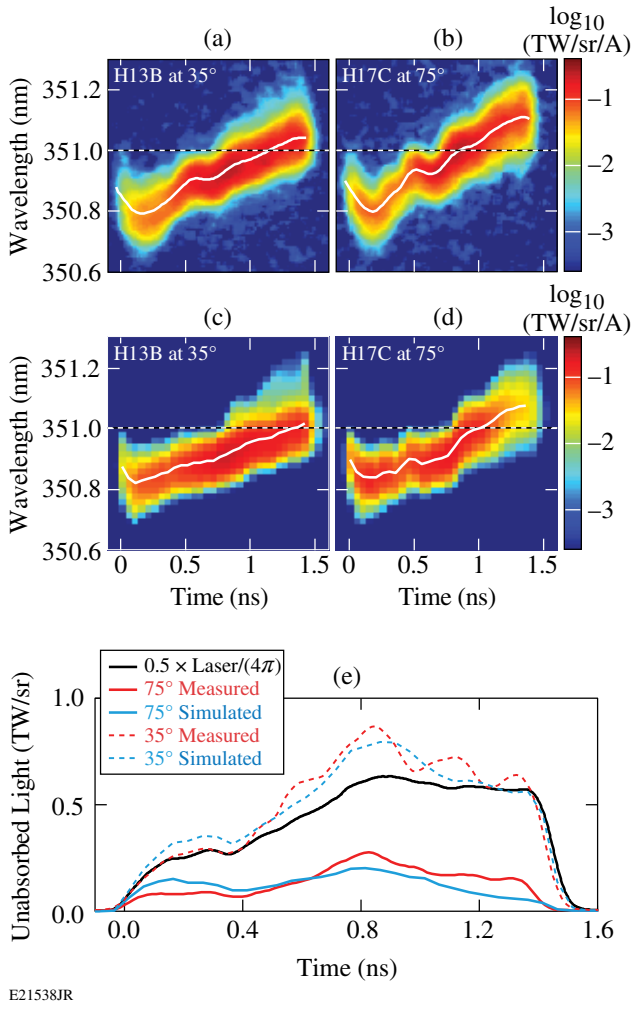

Figure 133.31
Unabsorbed laser light spectra measured at (a) 35° and (b) 75° from the PD pole along with the respective simulated spectra [(c) and (d)]. (e) The time-varying radiant intensity of the measured (red curves) and simulated (blue curves) unabsorbed laser light. Shown for reference is the radiant intensity that would result if the total incident laser power (black curve) were spread evenly over 4π steradian (divided by 2 for convenient scaling).

Figures 133.31(c) and 133.31(d) show the time-varying spectral intensity calculated by the CBET model. The important features present in the measured spectra are reproduced, indicating the accuracy of the hydrodynamic modeling used to calculate coronal plasma conditions. The discrepancy in the magnitude of the initial blue shift in the spectra is similar to that observed for symmetric drive implosions when a flux-limited heat-transport model was used. A nonlocal electron-transport model was required to accurately model the initial blue-shifted unabsorbed light for symmetric implosions.[9] The flux-limited model predicts shorter density scale-lengths than the nonlocal model, resulting in a slower initial outward movement of the plasma's critical-density surface and less coronal plasma density along the laser light's optical paths. Both effects decrease the predicted initial blue shift of the unabsorbed light spectrum.

The time-varying radiant intensity (TW/sr) of the unabsorbed light shown in Fig. 133.31(e) is obtained by integrating the spectra over wavelength. The calculations are in good agreement with the measurements. The accuracy of the scattered-light predictions given by the CBET model allows one to draw conclusions about the effect of CBET on the drive energetics during a PD implosion and to suggest possible CBET mitigation strategies.

Calculations indicate that CBET reduces the absorption from 85% to 76% and that this reduction is disproportionately distributed among the rings. The closer the ring is pointed to the equator, the more it is affected by CBET. The absorption in Ring 1 (the most-polar ring) drops to 82%, while Ring 3 (the most-equatorial ring) has its absorption reduced to 72% by CBET. This is consistent with the measured bang time being ~180 ps later than predicted when CBET is not included in the hydrodynamics code.[14]

The location where CBET occurs in PD is illustrated in Fig. 133.32. For all three beam rings, CBET results in a net loss of energy from the center portion of the beam profiles. This central portion includes the beamlets with the smallest impact parameters that penetrate farthest into the coronal plasma. In

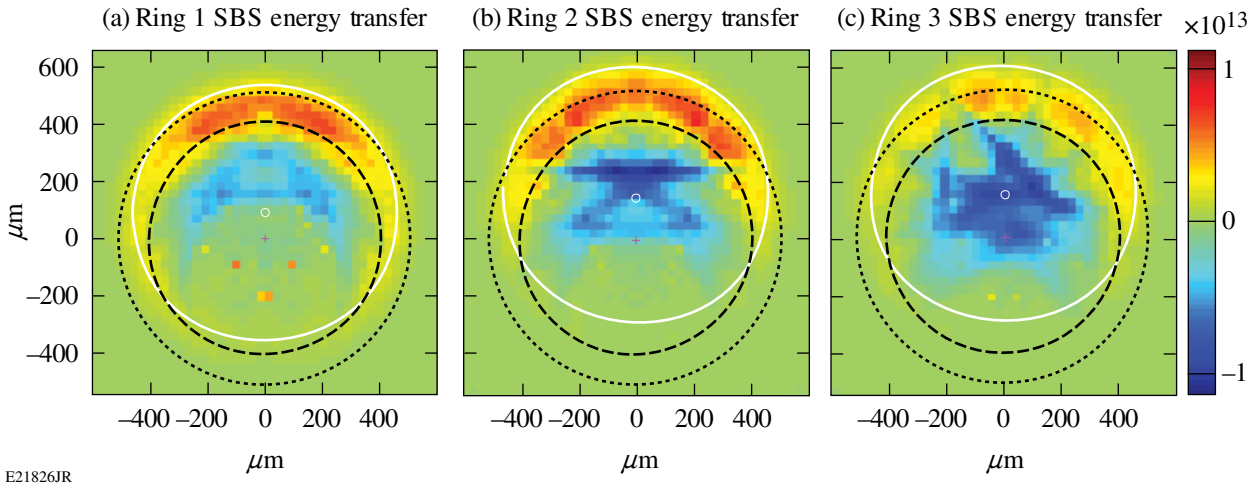

Figure 133.32
The normalized energy transferred for each OMEGA PD beam ring: (a) Ring 1, (b) Ring 2, and (c) Ring 3. The position of each pixel is the launch point of a beamlet, the sum of which represents the beam profile of one of the beams in an OMEGA PD beam ring. The magnitude of each pixel is the relative net energy transferred into (positive/red) or out of (negative/blue) a beamlet integrated along the path of each beamlet. The black curves show the position of the target's critical surface (dashed) and quarter-critical surfaces (dotted) with respect to the launched position of the beamlets. The white curve is the 95% power contour of the laser-beam spot.

the absence of CBET, these beamlets deposit their energy closest to the ablation surface and would most efficiently drive the target. In contrast, beamlets with impact parameters outside the plasma's critical-density radius gain a net amount of energy from CBET but are less efficiently absorbed. In effect, energy is transferred from the drive-efficient, small-impact-parameter beamlets to the less-efficient, higher-impact-parameter beamlets, resulting in reduced hydrodynamic efficiency.

The distribution of CBET over the beam profiles suggests a possible strategy to reducing its detrimental effect on driving the target: eliminating the high-impact-parameter beamlets that "steal" energy from the drive-efficient beamlets. The CBET model predicts that for the coronal plasma conditions in the OMEGA PD implosions, the overall absorption loss to CBET can be recovered using 30%-smaller beam radii. This improvement comes from a combination of reducing CBET and concentrating the beam energy into the more-efficient, low-impact-parameter beamlets. The effect of smaller spot sizes on implosion symmetry should be studied because PD implosions require some high-impact-parameter beamlets to direct energy toward the equator for symmetry.

Figure 133.33 illustrates the effect that varying the wavelength of the laser beams has on the energy absorbed from each ring. The predicted CBET among the rings is altered when laser

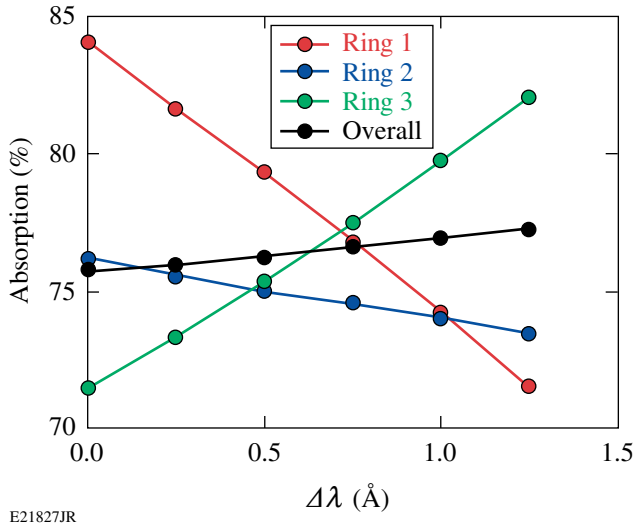

Figure 133.33
The absorption in each PD ring varies significantly when there is a difference in wavelength between the rings. Here $\Delta\lambda$ is the separation in wavelength between the rings. For example if $\Delta\lambda = 1$ Å, the wavelength of Ring 3 is 1 Å greater than Ring 2, which has a wavelength 1 Å greater than Ring 1.

beams of different rings have different wavelengths. The flow of energy is biased toward the beams in the rings with the longer wavelengths. When the wavelengths of the beams in all rings are equal ($\Delta\lambda = 0$), CBET between the beams in Rings 1 and 3

results in a net gain for the beams in Ring 1 and a net loss for Ring 3 beams. As the wavelength separation between the beams in different rings increases (with Ring 3's wavelength growing larger than Ring 1's), the net transfer between Rings 1 and 3 is reduced and eventually reverses until the beams in Ring 3 experience a net gain in energy from CBET with beams in Ring 1. At wavelength shifts greater than ~0.75 Å, the absorbed energy from beams in Ring 3 is greater than that from beams in Ring 1. The change in absorption for beams in Ring 2 is less pronounced. As $\Delta\lambda$ increases, the beams in Ring 2 take more energy from beams in Ring 1, which is offset by losing energy to beams in Ring 3. The overall energy absorption is nearly constant as $\Delta\lambda$ increases because gains by one ring are offset by losses in another. These results suggest that the power balance of the rings in a PD implosion can be controlled by independently setting the wavelengths of the rings with wavelength separations of the order of 1 Å (Ref. 7). This makes it possible to control the symmetry of a PD implosion.

In summary, measurements of the angular dependence of the unabsorbed light during polar-drive implosions at the Omega Laser Facility have been recorded. The radiant intensity of the unabsorbed light decreases from 1200 J/sr on the pole to 200 J/sr along the equator. The measured unabsorbed light intensity and spectrum are in good agreement with predictions from a 3-D CBET model. The modeling shows that CBET reduces the overall laser absorption in PD by ~10%. The ring of beams directed toward the PD equator is compromised most severely. The modeling provides insight into two possible CBET mitigation strategies. The location where the energy transfer occurs suggests that reducing the spot size will reduce the CBET losses. This is supported by modeling with small spot sizes where the laser absorption increased by ~10%. The modeling shows that the flow of energy between the PD beam rings can be manipulated by varying the wavelength separation between the rings. This could be used to regulate the power balance between the rings and exert control over the implosion symmetry. These results will help guide upcoming polar-drive experiments on the NIF, where 1.5 MJ of laser energy will be used to implode ~2-mm-diam capsules with the ultimate goal of producing fusion.[4]

ACKNOWLEDGMENT

We acknowledge the OMEGA operations team whose efforts enabled us to perform these polar-drive experiments. This work was supported by the U.S. Department of Energy Office of Inertial Confinement Fusion under Cooperative Agreement No. DE-FC52-08NA28302, the University of Rochester, and the New York State Energy Research and Development Authority. The support of DOE does not constitute an endorsement by DOE of the views expressed in this article.

REFERENCES

1. J. Nuckolls, L. Wood, A. Thiessen, and G. Zimmerman, Nature **239**, 139 (1972); V. N. Goncharov, T. C. Sangster, T. R. Boehly, S. X. Hu, I. V. Igumenshchev, F. J. Marshall, R. L. McCrory, D. D. Meyerhofer, P. B. Radha, W. Seka, S. Skupsky, C. Stoeckl, D. T. Casey, J. A. Frenje, and R. D. Petrasso, Phys. Rev. Lett. **104**, 165001 (2010).
2. E. I. Moses, Fusion Sci. Technol. **44**, 11 (2003).
3. S. Skupsky, J. A. Marozas, R. S. Craxton, R. Betti, T. J. B. Collins, J. A. Delettrez, V. N. Goncharov, P. W. McKenty, P. B. Radha, T. R. Boehly, J. P. Knauer, F. J. Marshall, D. R. Harding, J. D. Kilkenny, D. D. Meyerhofer, T. C. Sangster, and R. L. McCrory, Phys. Plasmas **11**, 2763 (2004).
4. T. J. B. Collins, J. A. Marozas, K. S. Anderson, R. Betti, R. S. Craxton, J. A. Delettrez, V. N. Goncharov, D. R. Harding, F. J. Marshall, R. L. McCrory, D. D. Meyerhofer, P. W. McKenty, P. B. Radha, A. Shvydky, S. Skupsky, and J. D. Zuegel, Phys. Plasmas **19**, 056308 (2012).
5. C. J. Randall, J. R. Albritton, and J. J. Thomson, Phys. Fluids **24**, 1474 (1981).
6. P. Michel *et al.*, Phys. Rev. Lett. **102**, 025004 (2009).
7. P. Michel *et al.*, Phys. Rev. E **83**, 046409 (2011).
8. W. Seka, D. H. Edgell, J. P. Knauer, J. F. Myatt, A. V. Maximov, R. W. Short, T. C. Sangster, C. Stoeckl, R. E. Bahr, R. S. Craxton, J. A. Delettrez, V. N. Goncharov, I. V. Igumenshchev, and D. Shvarts, Phys. Plasmas **15**, 056312 (2008).
9. I. V. Igumenshchev, D. H. Edgell, V. N. Goncharov, J. A. Delettrez, A. V. Maximov, J. F. Myatt, W. Seka, A. Shvydky, S. Skupsky, and C. Stoeckl, Phys. Plasmas **17**, 122708 (2010).
10. I. V. Igumenshchev, W. Seka, D. H. Edgell, D. T. Michel, D. H. Froula, V. N. Goncharov, R. S. Craxton, L. Divol, R. Epstein, R. Follett, J. H. Kelly, T. Z. Kosc, A. V. Maximov, R. L. McCrory, D. D. Meyerhofer, P. Michel, J. F. Myatt, T. C. Sangster, A. Shvydky, S. Skupsky, and C. Stoeckl, Phys. Plasmas **19**, 056314 (2012).
11. D. H. Froula, I. V. Igumenshchev, D. T. Michel, D. H. Edgell, R. Follett, V. Yu. Glebov, V. N. Goncharov, J. Kwiatkowski, F. J. Marshall, P. B. Radha, W. Seka, C. Sorce, S. Stagnitto, C. Stoeckl, and T. C. Sangster, Phys. Rev. Lett. **108**, 125003 (2012).
12. S. H. Glenzer *et al.*, Science **327**, 1228 (2010).
13. P. Michel *et al.*, Phys. Plasmas **17**, 056305 (2010).
14. P. B. Radha, J. A. Marozas, F. J. Marshall, A. Shvydky, T. J. B. Collins, V. N. Goncharov, R. L. McCrory, P. W. McKenty, D. D. Meyerhofer, T. C. Sangster, and S. Skupsky, Phys. Plasmas **19**, 082704 (2012).
15. P. B. Radha, V. N. Goncharov, T. J. B. Collins, J. A. Delettrez, Y. Elbaz, V. Yu. Glebov, R. L. Keck, D. E. Keller, J. P. Knauer, J. A. Marozas, F. J. Marshall, P. W. McKenty, D. D. Meyerhofer, S. P. Regan, T. C. Sangster, D. Shvarts, S. Skupsky, Y. Srebro, R. P. J. Town, and C. Stoeckl, Phys. Plasmas **12**, 032702 (2005).

16. R. C. Malone, R. L. McCrory, and R. L. Morse, Phys. Rev. Lett. **34**, 721 (1975).

17. J. Myatt, A. V. Maximov, W. Seka, R. S. Craxton, and R. W. Short, Phys. Plasmas **11**, 3394 (2004).

18. T. R. Boehly, V. A. Smalyuk, D. D. Meyerhofer, J. P. Knauer, D. K. Bradley, R. S. Craxton, M. J. Guardalben, S. Skupsky, and T. J. Kessler, J. Appl. Phys. **85**, 3444 (1999).

19. Y. Lin, T. J. Kessler, and G. N. Lawrence, Opt. Lett. **20**, 764 (1995).

20. S. Skupsky, R. W. Short, T. Kessler, R. S. Craxton, S. Letzring, and J. M. Soures, J. Appl. Phys. **66**, 3456 (1989).